

INVESTIGATION OF TAL OPTICAL EMISSIONS

G.F. Karabadzhak and A.V. Semenkina, Central Research Institute of Machine Building (TsNIIMASH), Korolev, Moscow Region, Russia; S.O. Tverdokhlebov, TsNIIMASH-EXPORT, Korolev, Moscow Region, Russia; and D.H. Manzella, NYMA Inc. NASA LeRC, OH, USA

Abstract

Optical emissions of three different xenon operating anode layer Hall thrusters (TAL) have been measured in the range of $\lambda=2600-11000$ Angstroms. Several tens of discharge as well as plume radiation spectra were obtained in various conditions of the TALs operation. Spectra taken at different time, but at the same condition appeared to be identical to the extent of the measurement accuracy, indicating stable performance of the thrusters. More than 430 individual transitions of XeI, XeII and XeIII have been identified in the spectra. Some strong lines of the erosion products have been detected in specially dedicated experiments. The emissions behavior have been investigated in different regimes of TAL operation. Plume radiance decay downstream the plume have been measured. Implementation of optical diagnostics for TAL performance evaluation and future plans are also discussed. The experiments and the data analysis are underway.

Introduction

Hall thrusters with closed electron drift, such as the TAL developed at TsNIIMASH, are increasingly being considered for different spacecraft propulsion requirements. The mission and integration requirements for these various applications are varied. In order to confirm the utility of anode layer thrusters to meet these requirements various experimental and analytic tools are available. This investigation considers the suitability of emission spectroscopy as a diagnostic tool for evaluating mission and integration requirements of anode layer thrusters as was previously done for stationary plasma thrusters¹.

Previous investigation of TAL emissions at TsNIIMASH have been done on TALs operating on propellants other than Xe (Li, Bi, Cs, Ar), therefore we had no any radiation spectral data from Xe operating TAL. From the other hand, past investigations of the stationary plasma Hall thrusters (SPT) using emission spectroscopy have demonstrated the possibility of non-intrusively evaluating the xenon plasma composition and estimating the optical contamination produced by thruster operation¹⁻⁴. During this study these aspects of the anode layer thruster operation were evaluated at TsNIIMASH using a new experimental system which was developed expressly for this purpose. Additionally, topics that were considered during this investigation were how the optical emission from anode layer thrusters changed with operating conditions and if

emission spectroscopy could be used as a real time, non-intrusive erosion diagnostic. Future plans for extending this diagnostic for evaluating the plasma state within the anode layer thruster are also discussed.

Apparatus and procedure

The optical measurements have been carried on concurrently with TAL performance tests. The TsNIIMASH test facility where the tests are performed as well as the test procedure are described elsewhere (see Carner, C.E at al, for instance)⁵. The vacuum chamber is now equipped with a quartz window, giving an opportunity to work in the UV region of spectrum. An illustrative sketch of the experimental set up is given in fig.1. Three different TALs, D-38, D-55 and D-100 have been tested. All of them used xenon as the propellant. General characteristics of the TALs as well as detailed information about their design and performance characteristics may be found in literature^{4,7}.

Two acousto-optical spectrometers were used for spectral measurements in most experiments. Some spectra were taken with the use of traditional grating monochromator followed by photomultiplier. The dispersing element which substitutes optical grating in the acousto-optical spectrometers is a quartz monocrystal. High frequency acoustic wave is generated in the crystal setting up a periodical spatial oscillation of the refractive index. Light diffracted on this periodical structure gives constructive interference only when the phase synchronism condition (Bragg condition) takes place:

$$dk=K,$$

where dk is a difference between falling and scattered light wave vector, and K is the acoustic wave vector. Therefore, one can change the wavelength of the reinforced light by changing the acoustic wave frequency. Specifically in these experiments the use of the acousto-optical spectrometers was justified, because they were easier to handle, had no high orders spectra contamination and had better spectral resolution than available grating monochromator. However, side these spectrometers had a complex instrumental function and provided only discrete scanning of spectrum resulted from the acoustic wave frequency stepwise changing. Some characteristics of the spectrometers are given in Table 1.

All three spectrometers were calibrated across the standard radiation sources based on

tungsten ribbon lamp (visible and near IR region) and deuterium lamp (UV region). Normally one spectrum per about four minutes was measured as a reasonable compromise between limited time of experiment and acceptable signal to noise ratio.

Four different lines of sight were chosen for the spectral measurements (Fig.2). Discharge radiation was measured, when the spectrometer line of sight was set up at the first position, whereas plume radiation was measured at the positions 2,3 and 4. The lines of sight crossed the engine axis at 4.7, 15 and 22.6 cm from the exit plane. The reason for this was that at 4-5 cm a plume core has been developed stretching over approximately 15-20 cm downstream from D-55 and D-38 thruster exits. At this distance plasma flux is already formed in axis-symmetrical flow with pronounced maximum of current density at the axis⁴. Whereas, at the distances longer than 20-22 cm the plume glows uniformly.

Indeed, measured signals were integrals along the lines of sight. But in course of the discharge radiation measurements most contribution to the signal came from the discharge itself. The plume radiation measurements at the closest to the discharge region (line 2 in fig.2) mostly affected by a small centimeter scale core region located at the axis. Yield from the peripheral regions of the plume was negligible here. For the line-of-sight 3 radiation collected from peripheral regions could impact the signal to some extent. And for the line 4 the signal essentially was an integral along the line-of-sight. In these experiments we had no a provision to move the lines-of-sight far enough off from the thruster axis. Therefore, utilization of the Abel conversion technique was not possible at this stage of the research.

Results and discussion

Most of the data were obtained from D-38 and D-55 engines so far. Just some spectra (mainly in the near IR region) have been taken from D-100 by now. Spectra taken at different times but at the same working conditions were identical to the extent of the measurement accuracy. This fact indicates stable performance of the thrusters. Figures 3 a, b and c represent typical discharge radiation spectra processed under assumption of the optically thin plasma. Spectral radiation per solid angle unit from the hole volume of the discharge is presented in these figures.

As it seen from the pictures the spectra overlap at the edges, so one can find the same lines in different spectra. The fact that the same lines

may have different heights in Figs.3a and 3b is resulted from different spectral resolutions of the spectrometers (see Table 1). Integral radiation in the spectral lines remains the same.

More than 430 lines of XeI, XeII and XeIII have been identified in the $\lambda=2600-11000$ Å spectral region. Most of them (about 260) were due to singly ionized XeII radiation. In the UV and visible region of spectrum the XeII emissions are dominant. Almost all detected XeIII lines were in the UV-region. IR radiation spectra practically consist of strong XeI emissions only. The most prominent Xe I lines, which can be easily found in a low temperature xenon plasma are comparable but weaker than strong Xe II lines in the TAL discharge plasma. Doubly ionized Xe III emissions in the UV region are comparable with those of XeII. Among other species emission of OI ($\lambda=7774.2$ Å) manifold was recognized in almost all spectra. Hydrogen H₂ ($\lambda=6562.8$ Å) line as well as some strong lines of erosion products have been detected in dedicated experiments. However, some features presumably not related with xenon atomic and ionic transitions still remain unidentified. The spectra analysis is in progress.

Comparison of the TAL spectra with the SPT-100 spectra¹ shows a great deal of similarity between them. Relative intensity of the TAL emissions coincides practically with SPT-100 in visible region of spectrum. Discharge brightness of the D-55 thruster which has approximately the same power and thrust as the SPT-100 was estimated to be about 35 mW/cm². This value is reasonably higher than 31 mW/cm² inferred from the data obtained at SPT-100 thruster exit plane¹ and much lesser than the percentage of power input radiated in visible region reported for SPT thruster².

Radiation intensity in dependence on D-38 thruster power input was investigated at a constant Xe flow rate. Fig.4 shows the D-38 thruster VC curve. Operation modes where radiation spectra were taken are numerated from 1 to 9 in this figure. Points located at the right side from the curve maximum are considered as working points. On the opposite, those located at the left are considered as anomalous regime points. Plume looks essentially different here and spectral distribution of the radiation intensity changes significantly at the anomalous regime. In particular, it may be seen in fig.5, where relative intensities of some XeI and XeII lines at different operational points are represented.

In some experiments the possibility of TAL life time evaluation basing on the analysis of erosion products emissions was investigated. It was difficult to detect the emission of the erosion products in the TALs with external anode layer. Therefore, D-38 thruster with extended discharge chamber was used in these experiments. As the result some strong lines of the erosion products have been detected. As an example, the behavior of some CrI emissions is presented in fig.5 too.

Fig.5 indicates that behavior of the curves belonged to the Xe II is essentially different at the point 1 in comparison with those of Xe I. From the other side, in the working regime modes (points 2 to 9) all xenon lines exhibited similar behavior with a little difference between XeI and XeII, whereas behavior of the erosion products emissions was substantially different. One can see the Xe lines intensities grow with increase of the current, whereas Cr lines intensities fall down. This can be easily explained by the dependence of erosion coefficients on the ion energy³. As soon as the erosion coefficients decrease quite rapidly with the voltage in this region, even small voltage reduction related to the current growth (see fig.4) appears to be enough to result in the substantial decrease of the erosion. Once again, it should be stressed that these lines were not found in the spectra obtained from TALs with the external anode layer such as D-55⁷.

Fig.6 represents total discharge radiation power from the D-38 thruster in different modes of operation. The thruster power consumption and current curves are shown in this figure for comparison as well.

Experiments performed with different thrusters showed that their spectra are identically featured differing in absolute values. Exception were some minor features not related to xenon radiation. For example, intensities measured in D-38 radiation spectra at close to the nominal regime of operation ($U=303$ V, $I=2.55$ Amp.) were lesser in average than D-55 intensities, resulting in integral discharge radiation of 0.13 Watts in the visible region in comparison with 0.58 Watts for D-55 at nominal regime ($U=302$ V, $I=2.44$ Amp.) in the same wavelength region. It should be mentioned, however, that anode of the D-38 thruster was located in the depth of the thruster body, whereas the D-55 had external anode located practically at the exit plane. This made part of the D-38 discharge obscured by the thruster body in comparison with the D-55 where all discharge

volume could be observed from the spectrometer position.

Fig.7 shows radiation intensity evolution of selected XeI, XeII and XeIII lines from discharge downstream the plume. Upper level energies of the correspondent transitions are given in the round brackets⁹. As it is seen from fig.7 emissions from different species evolve in different ways. XeI emissions fall downstream the plume not as much rapidly as those of XeII and XeIII. Obviously, this may be resulted from the fact that concentration of neutral Xe atoms decreases downstream the plume not as much rapidly as that of ions. However, lines belonged to the same ion exhibit different behavior as well. In general, intensity of those lines falls more rapidly which have higher excitation potential. This fact may be considered as a complimentary evidence of a decrease of electron temperature downstream the plume⁴.

D-55 UV through visible integral radiation flux per centimeter plume length is shown in Fig.8. The flux values presented in this plot were derived from plume radiation spectral measurements along different lines of sight. For simplicity of the data representation the discharge radiation was averaged along the first centimeter length of the plume. Radial distributions of the plume plasma parameters including specific radiance were approximated by triangle functions with the maximum at the axis. Estimate of the FWHM (Full Width at Half Maximum) for these distributions was based on the available plume data⁴. To obtain total power value accumulated in the emitted radiation one has to integrate the flux value over the plume length. This might be useful to know for assessment of the thruster radiation impact on a spacecraft optical equipment. As it seen from fig.8 more than 90 percent of TAL radiation is concentrated in close to the thruster region of some centimeter scale.

Attempts have been made to observe oscillations of the TAL plasma radiation using filtered photomultipliers. No strictly pronounced periodical oscillations have been discovered in D-38 and D-55 thrusters radiation at close to nominal operating conditions. However, recorded signals indicated rather broad frequency spectrum in the region of tens kHz. Comparison with current signal showed that the radiation oscillation spectrum corresponds in general to the current oscillations.

Meanwhile, in the operating regimes which are close to the maximum of the discharge current on the VC curve a tendency had been

developed to the periodical oscillations appearance. This effect was expressed more for D-100 thruster, operating with high mass flow rate. In this case oscillations frequency changed roughly from 30 to 50 kHz depending on voltage, whereas signal modulation was of some tens percents. Study of the oscillation is underway.

Implementation of optical diagnostics for TAL performance evaluation.

Future work plans.

Optical diagnostics is traditionally considered as a powerful tool for determination of plasma parameters. Most of previous works related to Hall thrusters optical diagnostics have been performed on SPT devices^{1-3,10,11}. Of course, all diagnostic methods used in previous works are applicable for determination of the TAL plasma parameters too. However, to infer the parameters from measured spectra one has to make some preliminary assumptions about the plasma conditions. One of these assumptions is that the TAL discharge and plume plasmas are optically thin. This assumption looks reasonable for rarefied TAL plasma, indeed, as soon as even maximal absorption cross sections for atomic lines is much less than $1/NL$, where N is absorbing component concentration and L is plasma dimension along the line of sight. This allows emitted radiation to come freely out of the plasma without any absorption. Therefore, no need is to solve the radiation transfer equation. In this case measured radiation intensity resulted from atom (ion) transition from i -level to k -level is simply related with concentration of the excited atoms in i -state as:

$$4\pi I_{ik} = A_{ik} h\nu \Omega \int N_i^*(l) dl, \quad (1)$$

where A_{ik} -spontaneous radiation decay probability, l -distance along the spectrometer line of sight, $N_i^*(l)$ - concentration of atoms (ions) in i -state, $h\nu$ - energy of emitted light quantum, Ω -spectrometer field of view solid angle.

Next reasonable assumption would be one of TAL plasma axial symmetry. This assumption is based on the general design of axisymmetrical TALs. For such types of plasma the excited state concentration is determined from equation (1) by using Abel conversion technique. A set of measurements along different lines of sight located in perpendicular to the thruster axis plane is required for this. However, sometimes relatively small plasma regions can be found, which definitely provide most of contribution to the signal along the line of sight. Example is the measurement of radiation from a small but

intensively radiating discharge region through relatively low radiating plume. In this case contribution from the low radiating regions may be neglected and need vanishes in integration of the equation (1). Then the relation (1) provides the easiest way to determine the concentration of the excited species from measured intensity of radiation. The main uncertainties here are addressed to the radiation decay probabilities. Accuracy of our measurement of the radiation intensity was typically some percent for relative measurements and from 8 to 30 percent for absolute measurements.

To use equation (1) for calculation of the plasma parameters one has to consider the processes responsible for population and depopulation of the excited states. This question has been investigated before in the course of interpretation of experimental data obtained from SPT^{1-3,11}. We opine, that general approach to the plasma modeling developed for SPT is applicable for TAL too. The basic assumptions are as follows:

1. Atomic (ionic) levels with high principle numbers $n \geq n_0$ are in collisional equilibrium with free electrons in plasma. Population of these levels may be described by Boltzmann distribution formula with governing temperature T_e . Indeed, n_0 may vary from case to case, but in any case one can find a level starting from which Boltzmann statistics can be used to describe its population. Basis for this assertion is that probability of spontaneous radiation goes down, whereas collision cross section goes up with the growth of upper level principle number of the excited atom. Hence, starting from some level the probability of its collisional de-excitation becomes to prevail over others. Equilibrium condition in this case is used to call collisional-radiative equilibrium (CRE)^{12,13}. Radiation intensity under this condition is related to the plasma electron temperature trough:

$$\ln \frac{I_{ik}}{A_{ik} h\nu g_i} + const = -\frac{\mathcal{E}_i}{kT_e} \quad (2)$$

where \mathcal{E}_i - upper level energy, g_i statistical weight of the i -level. Being plotted versus \mathcal{E}_i the $\ln I_{ik}/A_{ik} h\nu g_i$ value must fall on a straight line. The electron temperature T_e can be determined from the slope of this line to the X-axis. The Boltzmann plots like this built for SPT plasma radiation¹ gave essential scattering in the electron temperature values. Taking into account similarity of TAL and

SPT-100 spectra, not surprising is that our quick look evaluation of the TAL discharge electron temperature gave the same result. This fact indicates that not all considering levels are in CRE. Reasonable would be to find quite high levels for which CRE model can be applied, but due to the low probability of the spontaneous decay, radiation from these levels would have relatively low intensity. Perhaps, desired signal to noise ratio could be gained from improving of radiation detecting technique. We plan to do this work in the nearest future.

2. *Corona equilibrium (CE) model*^{12,13} is assumed to be valid for atomic levels with small principal number n and high probability of spontaneous radiation decay. In this type of plasma equilibrium radiation intensity related with the plasma parameters as:

$$4\pi \sum_r \Sigma A_r = A_{ik} h \nu N_e N_0 \Omega L \int f_e(v) \sigma(v) dv \quad (3)$$

where N_e -electron concentration, N_0 -concentration of atoms (ions), $f_e(v)$ -electron velocity distribution function, $\sigma(v)$ - collisional excitation cross section of the xenon atoms (ions) by the electrons, and summation is made over all $r < i$.

Our estimate shows that in TAL discharge and plume plasmas (in the near field at least) electron-electron collision frequency is high enough for the electron thermalization. Due to inelastic collisions the velocity distribution, perhaps, may differ from the Maxwellian at high velocities, but the Maxwellian distribution may be used as a "zero level" approach in equation (3). For the Maxwellian distribution the plasma parameters are related with the measured radiation intensity through:

$$I_{ik} \sum A_{ik} = h \nu A_{ik} N_e N_0 \Omega L \left(\frac{m}{2\pi k T_e} \right)^{3/2} \times \int e^{-\frac{mv^2}{kT_e}} \sigma(v) v^3 dv \quad (4)$$

Relation (4) provides the way to determine any plasma parameter if CR model is applicable and the atomic (ionic) constants and other plasma parameters are known from elsewhere. When possible, the equations are solved together with charge conservation, energy/mass balance and other equations, which may be combined into the closed system.

TAL experimental data analysis showed that real TAL plasma spectra can't be modeled basing either CR or CRE model only. Stepwise

excitation from Xe metastable states can impact the excited states population in the CR model. From the other side population of the levels which are collisionally coupled with the resonant one and with those which are in turn coupled with lower levels through a strong allowed radiation transition appeared to be suppressed. As the matter of fact, for accurate determination of the TAL plasma parameters a full set of kinetic equations for each separate atomic (ionic) state must be solved. It is rather problematic task now. Therefore, attention should be paid to semi-phenomenological evaluation of the plasma parameters which are directly related to the engine performance and spacecraft integration issues.

Example might be the total and spectral radiation measurements for assessment of the radiation impact onto the spacecraft optical equipment as well as for evaluation of the radiation losses, which were reported taken off substantial part of the total power of the SPT thruster³. These values can be inferred directly from the radiation measurements without any further assumptions on the plasma condition.

Another example is the measurement of the erosion products emission for the thruster life time evaluation. High sensitivity and improved performance of the spectrometric instruments used in these work gave us a chance to study the evolution of the erosion product emission in the thruster which erosion rate is smaller than in SPT-100 tested before¹. Fig.9 shows average relative intensities of the CrI lines normalized to the dependence of the Cr erosion coefficient on voltage⁸. The chrome emissions behavior expectedly follows the xenon one, if the erosion coefficient/voltage dependence is taken into account. Separate detailed study of this question is planned in the nearest future for developing of life time evaluation procedure based on optical emissions measurement.

Conclusion

TAL discharge and plume radiation spectra have been measured in the wide wavelength region $\lambda=2650-11000$ A. More than 430 XeI, XeII and XeIII transitions were identified. Integral radiation power of 0.84 Watts was measured in the region $\lambda=2650-8000$ A from D-55 discharge in nominal regime of operation ($U=305$ V, $I=4,45$ A). About 70% of this value is visible radiation. Total plume radiation is more than order of magnitude less. The plume radiation rapidly decreases in some centimeters from the thruster

exit plane. Quick look analysis shows that it is mostly due to decreasing of the electron temperature downstream the plume. The investigation revealed promise in application of the optical diagnostics to TALs general performance and life time evaluation. Emissions of erosion products detected in some dedicated experiments on D-38 with extended discharge chamber give a basis for developing of a real time, non-intrusive erosion diagnostic of various Hall thrusters with closed electron drift.

Acknowledgment

These work was partially sponsored by NASA LeRC via Texas Tech. University. Authors would like to thank personally Dr. F.Curran, J.Sankovic and R.Jancovsky of NASA LeRC for their support of this investigation.

References

- Manzella, D.H., "Stationary Plasma Thruster Plume Emissions", IEPC-93-097, Proc. of 23 Int'l Electric Propulsion Conference, 1993, p.913.
- Bugrova, A.I., Ermolenko, V.A., Sokolov, A.S., "Optical Investigation of Neutral Component of Nonequilibrium Xenon Plasma", *Teplotfizika Vysokih Temperatur*, vol.25, No.6, Nov. 1987, p.1080.
- Bugrova, A.I., Ermolenko, V.A., Niskin, V.T., Sokolov, A.S., "Spectral characteristics of closed drift Hall thruster radiation energy", *Teplotfizika Vysokih Temperatur*, vol.19, No.2, 1981, p.428.
- Domonkos, M.T., Marrese, C.M., Haas, J.M., Gallimore, A.D., "Very Near-Field Plume Investigation of the D-55", AIAA-97-3062, 33rd AIAA/ASME/SAE/ASEE Joint Propulsion Conf., July 1997, Seattle, WA
- Garner, C.E., Tverdokhlebov, S.O., Semenkin, A.V., Garkusha V.I., "Evaluation of 4.5 kW D-100 Thruster with Anode Layer", AIAA-96-2967, 32nd AIAA/ASME/SAE/ASEE Joint Propulsion Conf., July, 1996, FL.
- Manzella, D.H., Oleson, S., Sankovic, J., Haag, T., Semenkin, A., Kim, V., "Evaluation of Low Power Hall Thruster Propulsion", AIAA-96-2736, 32nd AIAA/ASME/SAE/ASEE Joint Propulsion Conf., July, 1996, FL.
- Garner, C.E. et al., "Experimental Evaluation of Russian Anode Layer Thrusters", AIAA-94-3010, 30th AIAA/ASME/SAE/ASEE Joint Propulsion Conf., June, 1994, IN
- Pleshvtsev, N.V., "Sputtering processes", Moscow, 1968. (in Russian).
- Striganov, A.R. and Sventitskii, N.S., "Tables of Spectral Lines of Neutral and Ionized Atoms", Atomizdat, Moscow, 1966. (translation from Russian - IFI/Plenum, New York, 1968).
- Darnon, F., Lyszyk, A., Bouchoule, A., "Optical Investigation of Plasma Oscillations of SPT Thrusters", AIAA-97-3051, 33rd AIAA/ASME/SAE/ASEE Joint Propulsion Conf., July 1997, Seattle, WA
- Bugrova, A.I., Volkova, L.M., Ermolenko, V.A., Kral'kina, E.A., Dev'atov, A.M., Kharchevnikov, V.K., "Dynamics of the Electron Energy Distribution Function in a Plasma Accelerator with Extended Acceleration Zone", *Teplotfizika Vysokih Temperatur*, vol.19, No.6, Nov. 1981, p.1149.
- McWhiter, R.W.P., "Spectral Intensities", in "Plasma Diagnostic Techniques", ed. by Huddleston, R.H. and Leonard, S.L., Academic Press, New York-London, 1965.
- Griem, H.R., "Plasma Spectroscopy", New York-San Francisco-Toronto-London, 1964.

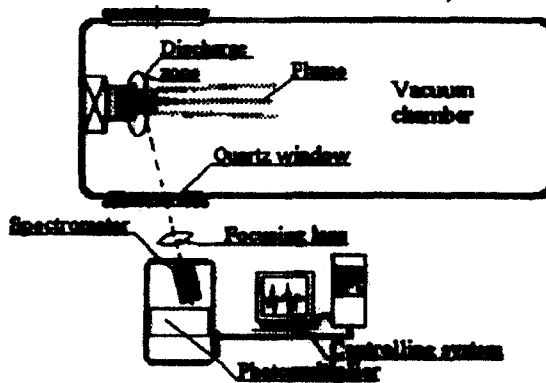


Fig. 1. Experimental set up diagram

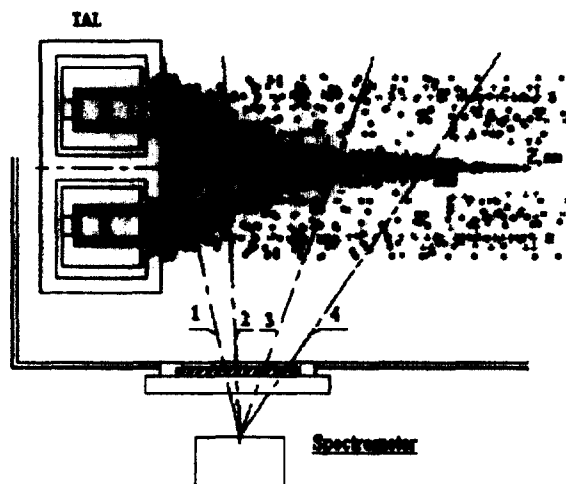


Fig. 2. Spectrometer lines of sight

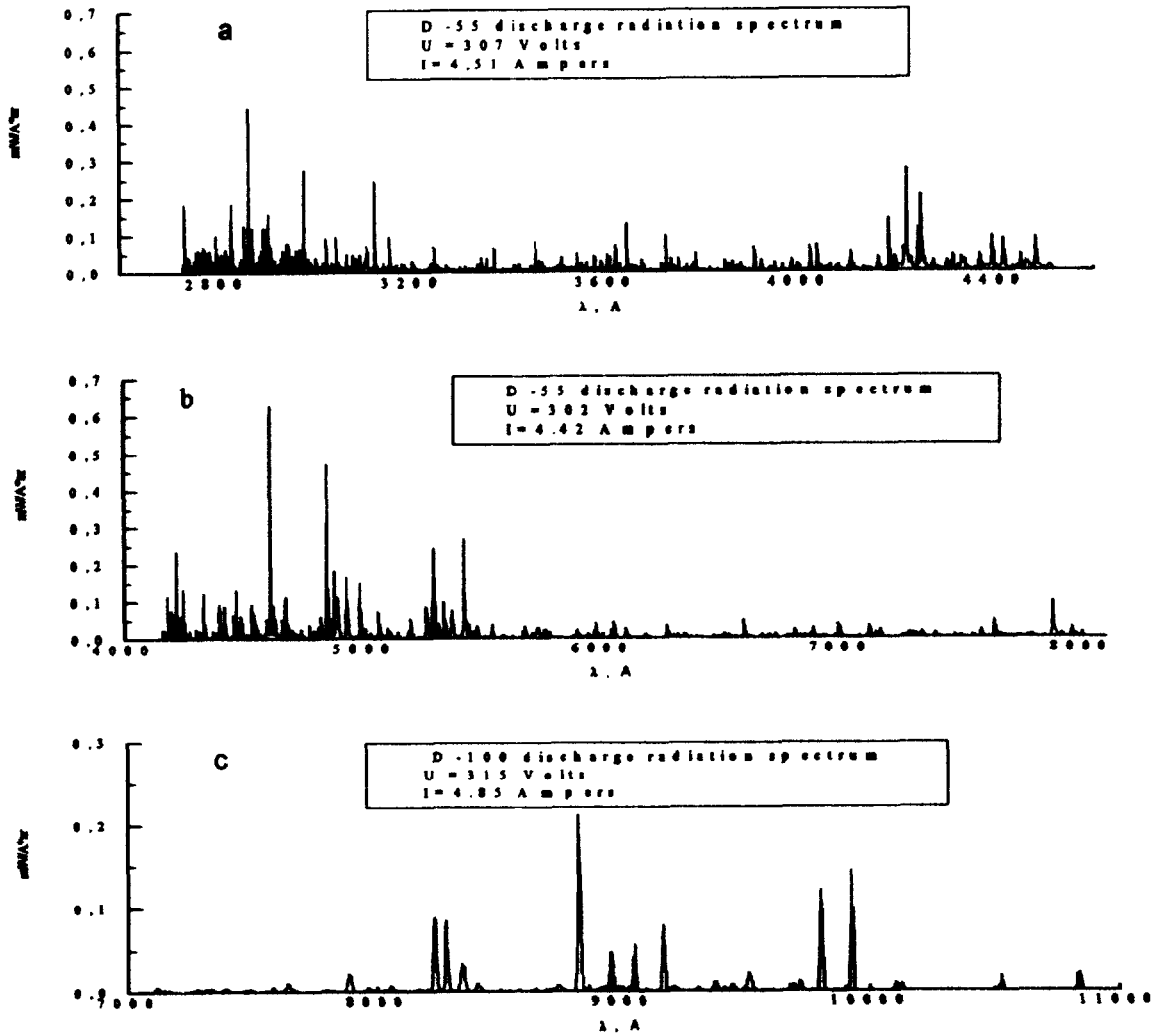


Fig.3 a-c. Typical TAL discharge radiation spectra.

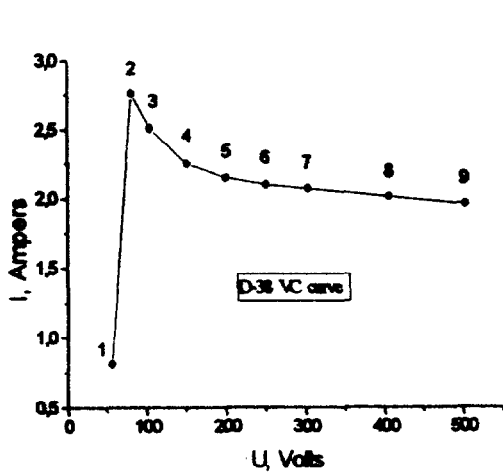


Fig.4. D-38 thruster VC curve. Circles indicate the operating points where radiation spectra were taken.

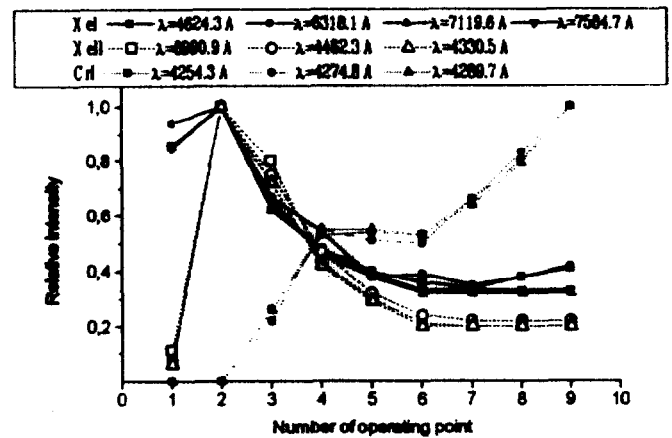


Fig.5. Behavior of some D-38 discharge emissions depending on operating condition. Numbers on the X-axis correspond to the operating points in fig.4.

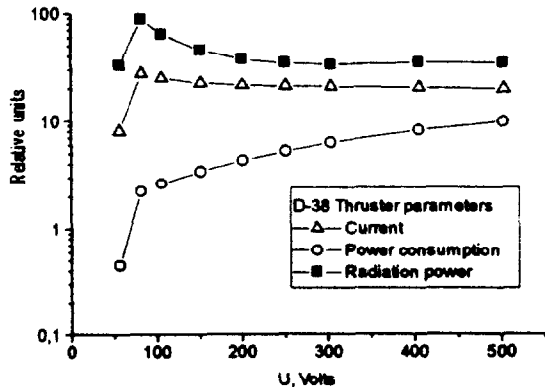


Fig. 6. Comparison of D-38 thruster radiation power with its current and power consumption

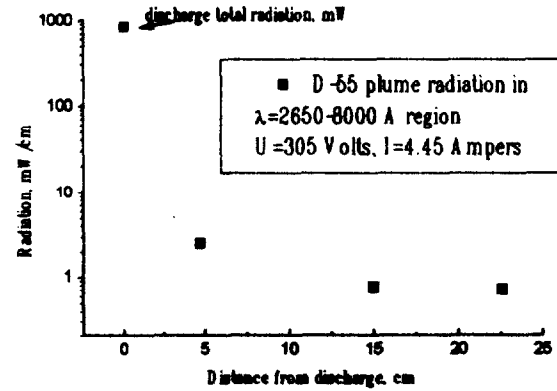


Fig. 8. Total radiation power per centimeter length of the D-55 plume. Arrow pointed data is total discharge radiation. U=305 V, I=4.45 A

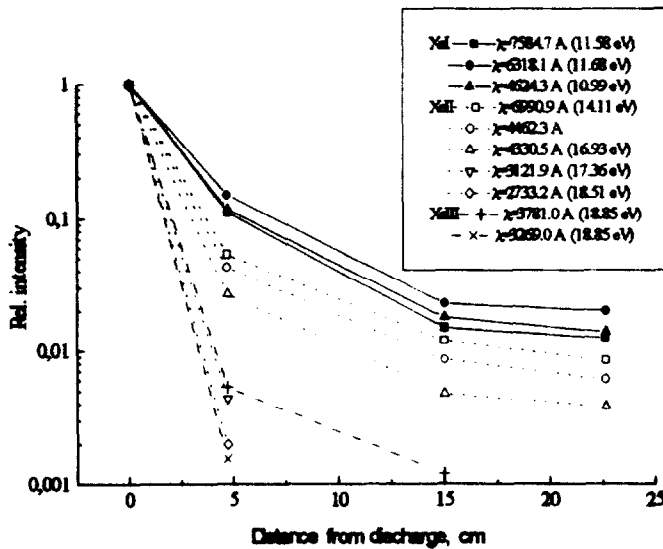


Fig. 7. Evolution of radiation of some Xe lines downstream the plume. Upper level energy is given in brackets⁹.

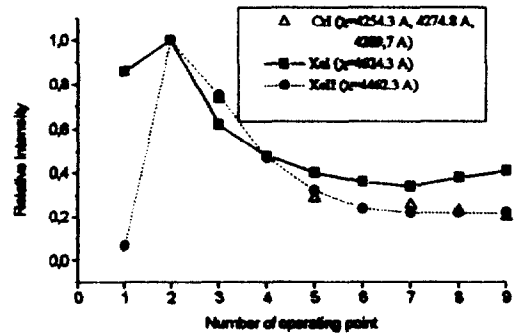


Fig. 9. Average relative radiation intensity of three CrI lines normalized to Cr erosion coefficient voltage dependence. XeI and XeII lines are given for comparison as well.

Table 1. Spectrometer characteristics

Type of spectrometer	Wavelength region, A	Spectral resolution, A	Aperture	Scanning step
Visible acousto-optical monochromator followed by photomultiplier	4150-8000	2-3 in the blue region 5-7 in the red region	6 mm diameter, 1/30 radian solid angle	2048 points per spectrum
UV acousto-optical monochromator followed by photomultiplier	2650- 4400	2 at short wavelengths 4-5 at long wavelengths	6 mm diameter, 1/30 radian solid angle	2048 points per spectrum
Asymmetrical Fastie grating monochromator followed by photomultiplier	7000-12000	15.6 FWHM at 0.3 mm width slits	F=600 mm 1:8 rel. aperture	continuous scanning